Role of attached polymer chains on the vibrational relaxation of a C_{60} fullerene in aqueous solution

Hojin Kim, Dmitry Bedrov, and Grant D. Smith
Department of Materials Science and Engineering and Department of Chemical Engineering, University of Utah, Salt Lake City, Utah 84112, USA

Sergei Shenogin and Pawel Keblinski
Department of Materials Science and Engineering, Rensselaer Polytechnic Institute, Troy, New York 12180, USA
(Received 29 March 2005; published 25 August 2005)

We have investigated the vibrational relaxation of a bare C_{60} fullerene and C_{60} fullerenes with covalently attached poly (ethylene oxide) (PEO) chains in aqueous solution using classical molecular dynamics simulations. The rate of transfer of vibrational energy from the excited fullerene to the surrounding water was found to be slow for the bare fullerene, with a vibrational relaxation time of approaching 200 ps. Attachment of a single short PEO chain (M_W=250), yielding C_{60}-PEO, was found to decrease the vibrational relaxation time by about a factor 5, while the vibrational relaxation time for a fullerene with six attached PEO chains, or C_{60}-$(PEO)_6$, exhibited approximately 25 times faster vibrational relaxation than the bare fullerene. The temperature of the attached PEO chain(s) was found to increase during the vibrational relaxation of the fullerene, but remained well below that of the fullerene, indicating that the rate limiting step in vibrational relaxation of C_{60}-PEO is energy transfer from the fullerene to the attached PEO.

DOI: 10.1103/PhysRevB.72.085454 PACS number(s): 61.48.+c, 63.22.+m, 65.80.+n

I. INTRODUCTION

Photoexcited fullerenes have been the subject of much interest in recent years, both fundamental and applied.[1] Relaxation of laser excited C_{60} thin films[2–6] and toluene suspensions of C_{60},[7–11] C_{70},[7] and C_{76} and C_{84} (Ref. 12) yielded relaxation times on the order of 40 ps with all of the authors attributing the relaxation to a decay or transport property of the electronic system. Recently a combination of experimental and molecular dynamics studies have strongly suggested that the time evolution of the optical absorption is a signature of the vibrational relaxation of fullerene molecules, not the decay of electronic excited states.[13] In view of this finding, understanding the transport of energy between fullerenes and their surrounding matrix is central to understanding the vibrational relaxation of photoexcited particles and hence is important for many envisioned applications of fullerenes that seek to take advantage of this property of fullerenes.

In contrast to previous experimental and modeling work focused on fullerene suspensions in low polarity solvents, in this work we study the vibrational relaxation (cooling) of thermally excited C_{60} fullerenes in aqueous solution. For this purpose we have utilized classical molecular dynamics simulations to study vibrational relaxation from a single thermally excited fullerene in water with and without attached poly (ethylene oxide) (PEO) chains. PEO is commonly attached to fullerenes to prevent aggregation in aqueous solutions as well as to impart biocompatibility for *in vivo* biomedical applications.[14] Our recent simulations have demonstrated that attachment of short PEO oligomers can dramatically change the nature of C_{60} aggregation[15] in aqueous solution and can result in their dissolution.[16]

II. METHODOLOGY

All simulations were performed using the molecular dynamics simulation package Lucretius.[17] Simulations were performed on a bare C_{60} fullerene as well as fullerenes with one or six PEO chains (M_w=250) covalently to the fullerene as a C—O bond as illustrated in Fig. 1. Table I provides details of system configurations while Table II provides details of the interaction potentials employed in the simulations. A time step of 3 fs was used in all simulations with a truncation of nonbonded dispersion interactions at 10 Å. The particle mesh Ewald method[18] was used to handle long range Coulomb interactions. Equilibration was carried out using a cubic cell in the NPT ensemble at 298 K for 600 ps to yield equilibrium density at 1 atm pressure. The corresponding cell sizes are given in Table I.

Following equilibration, the fullerene vibrational temperature was instantaneously increased to 600 K by scaling the internal kinetic energy of the fullerene such that the total instantaneous vibrational energy, given as the sum of potential and kinetic contributions, was equal to the average vibrational energy for a C_{60} fullerene at 600 K as determined from simulations of a single unmodified fullerene at 600 K. Numerous sampling runs in the NVE ensemble, as detailed in Table I, were performed in order to monitor the vibrational relaxation of the fullerene. Each starting configuration for each fullerene NVE simulation was obtained from an *NVT* simulation of the corresponding system at 298 K separated by 100 ps of NVT simulation.

III. RESULTS AND DISCUSSION

A. Fullerene temperature and vibrational relaxation

The fullerene temperature $T_{C_{60}}$, averaged over the number of sampling runs as given in Table I, is shown for C_{60},

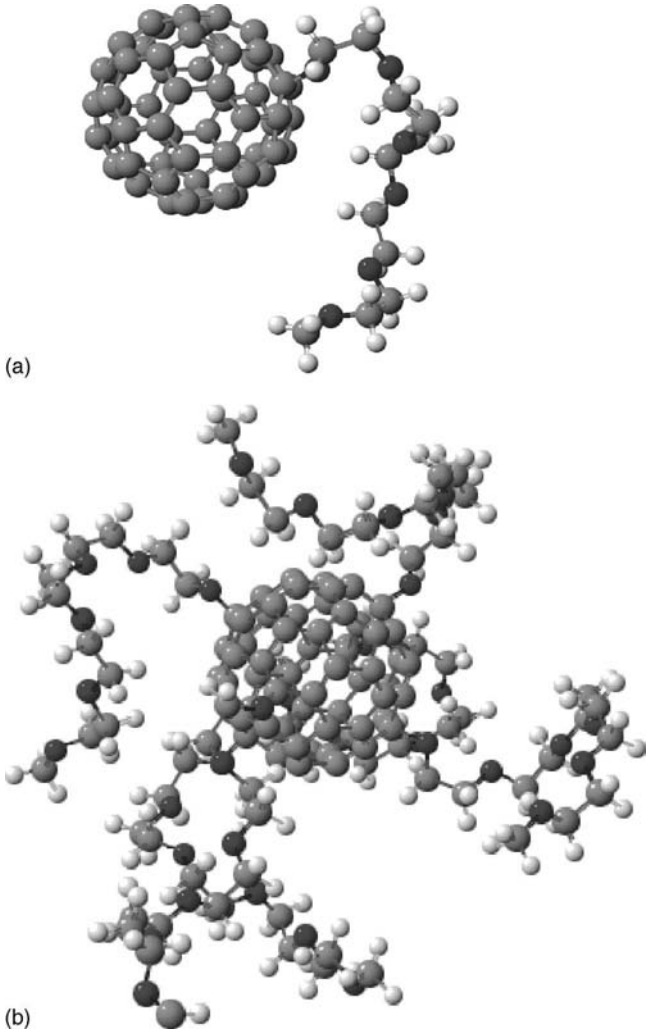

FIG. 1. Schematic of PEO modified fullerenes showing (a) one and (b) six attached PEO chains.

C_{60}-PEO, and C_{60}-$(PEO)_6$ in Fig. 2(a) as a function of time after excitation of the fullerene. It is clear that vibrational relaxation (cooling) of the fullerene occurs much more rapidly when PEO chains are covalently attached. Figure 2(b) shows $[T_{C_{60}}-T_{C_{60}}(eq)]/[T_{C_{60}}(0)-T_{C_{60}}(eq)]$ where $T_{C_{60}}(eq)$ is the equilibrium temperature of the fullerene after a long time (complete vibrational relaxation) and $T_{C_{60}}(0)$ is the temperature after vibrational excitation. The temperature decay can be represented reasonably well for each system with an exponential of the form

$$\frac{T_{C_{60}}-T_{C_{60}}(eq)}{T_{C_{60}}(0)-T_{C_{60}}(eq)}=A\exp[-t/\tau] \tag{1}$$

with relaxation times τ given in Table III. The preexponential factor A was very close to unity except for the bare fullerene where a value of 0.73 was obtained after excluding a transient period covering the first 30 ps of cooling from the fit. Assuming that the thermal relaxation is limited by the heat flow across the interface, the interfacial conductance, G, is given by[13]

$$G=\frac{C}{A\tau}, \tag{2}$$

where C is the heat capacity of the fullerene and A in the surface area of the fullerene based on the diameter of the carbon shell, ~6.8 Å, giving $A\sim 170$ Å^2, is also given in Table III for each system. The heat capacity, 0.177 kcal/mol/K,[19] was determined by performing simulations of a fullerene over a range of temperatures. While the heat capacity and vibrational relaxation time are a function of the number of classical degrees of freedom included for the fullerene, the interfacial conductance is not.[20] The interfacial conductance obtained for the bare C_{60} fullerene in water is about factor of 2 smaller than was found in comparable simulations of a C_{84} fullerene in alkane solvent where a value of 10 MW m^{-2} K^{-1} was obtained[13] (see Sec. IV for discussion).

TABLE I. Configuration of C_{60}/water systems.

System	Cell size (Å)	Number of water	Length of run (ns)	Number of runs
C_{60}	22.1139	340	1	40
C_{60}-PEO	22.3420	340	1	40
C_{60}-$(PEO)_6$	23.4277	340	1	40

B. Water temperature

Figure 3(a) shows the average temperature of the water solvent as a function of time during the fullerene cooling

TABLE II. Force fields utilized in molecular dynamic simulations.

Interaction	Source	References	Comments
C_{60} intramolecular		27–29	Bonds are constrained
PEO intramolecular	Quantum chemistry	30	Bonds are constrained
PEO-PEO	Empirical	30	
Water	TIP4P	31	Rigid molecule
C_{60}-PEO	Lorentz-Berthelot mixing rules	32	
C_{60}-water	Quantum chemistry/empirical	33	
PEO-water	Quantum chemistry	30	

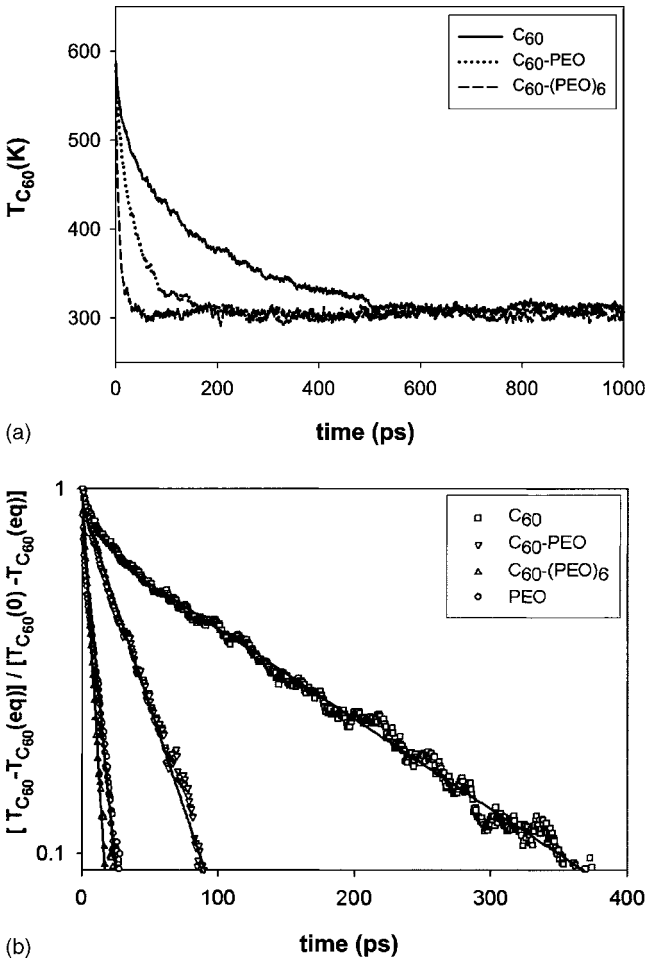

FIG. 2. (a) The fullerene temperature $T_{C_{60}}$ for C_{60}, C_{60}-PEO, and C_{60}-$(PEO)_6$ aqueous solutions during the fullerene cooling process. (b) Normalized temperature offset for fullerenes in C_{60}, C_{60}-PEO and C_{60}-$(PEO)_6$ in aqueous solution during the fullerene cooling process as well as that for relaxation of excited PEO in aqueous solutions of free PEO chains. Solid lines indicate the exponential decay [Eq. (1)].

process. Little temperature increase in the water is seen as the total heat capacity of the 340 water molecules is much greater than that of the single fullerene. The water temperature rises more rapidly for the PEO modified fullerenes compared to the bare fullerene, consistent with the increased interfacial conductance for these materials, with the rate of water temperature increase being greater for C_{60}-$(PEO)_6$ than for C_{60}-PEO.

Figures 3(b)–3(d) compare the temperature of the first hydration shell of water, based upon the C_{60}-water pair distribution function shown in the inset of Fig. 3(b), with that of the water solvent (all water). In all cases no difference can be seen between the temperature of the first water hydration shell and the overall water temperature. For the bare fullerene, this indicates that heat transfer through the liquid water occurs much more readily than transfer of energy to the interfacial water from the fullerene. For the PEO modified fullerenes, where vibrational cooling occurs primarily by transfer of vibrational energy from the fullerene to the PEO chain(s) and then to the water (see below), transfer of energy to the water does not occur primarily to the first hydration shell of the fullerene but rather to the water hydrating the PEO chain(s), which extend well beyond the first hydration shell into the water solvent.

TABLE III. Vibrational relaxation times and interfacial conductance in aqueous solution.

System	τ (ps)	G(MW m^{-2} K^{-1})
C_{60}	176	4
C_{60}-PEO	39	18
C_{60}-$(PEO)_6$	7	102
PEO	11	

C. Role of attached PEO in vibrational relaxation of C_{60}

It is clear that covalently attaching PEO significantly augments the vibrational relaxation of the C_{60} fullerene. This is not unexpected given the known behavior of the relaxation of vibrationally excited polyatomic molecules in solvent from both experiment and simulation. It is known that energy is transferred from vibrationally excited polyatomics to the solvent first by fast intramolecular transfer from high frequency, excited harmonic degrees of freedom (e.g., stretches and bends) to anharmonic modes (e.g., torsions) which can couple effectively with the solvent through anharmonic nonbonded interactions.[21–24] The vibrational spectra of a fullerene, determined from the velocity autocorrelation function[25] is shown in Fig. 4(a). There is very little density of states for the fullerene below 200 cm^{-1}, i.e., in the range associated with torsional motion of typical organics and "soft phonons" associated with nonbonded interactions in typical liquids.[21,22] Note that increasing spectral density for the fullerene at low wave numbers is associated with rotational and center of mass motion of the fullerene, and not internal vibrations. The vibration spectra for water shown in Fig. 4(b) shows significant low-frequency contributions associated with soft phonons, as expected.

Figure 4(c) shows that attachment of PEO to the fullerene does not significantly change the vibrational spectra of the fullerene itself. However, Fig. 4(d) reveals that PEO does have significant density of states in the low frequency region (due largely to torsional modes) thought to be important for vibrational relaxation Figures 5(a) and 5(b) reveals that the attached PEO is excited during vibrational cooling of the fullerene, indicating that transfer of energy from the fullerene to the attached PEO is an important mechanism in accounting for the dramatic decrease in interfacial resistance for heat transfer from the fullerene to water with attachment of PEO (see Table III).

Finally, the fullerene, PEO and water temperatures are compared for (a) C_{60}-PEO and (b) C_{60}-$(PEO)_6$ in Figs. 5(a) and 5(b), respectively, during the vibrational cooling process. The temperature of the PEO chain(s) remains significantly below that of the fullerene during most of the vibrational cooling process, indicating that the primary resistance for

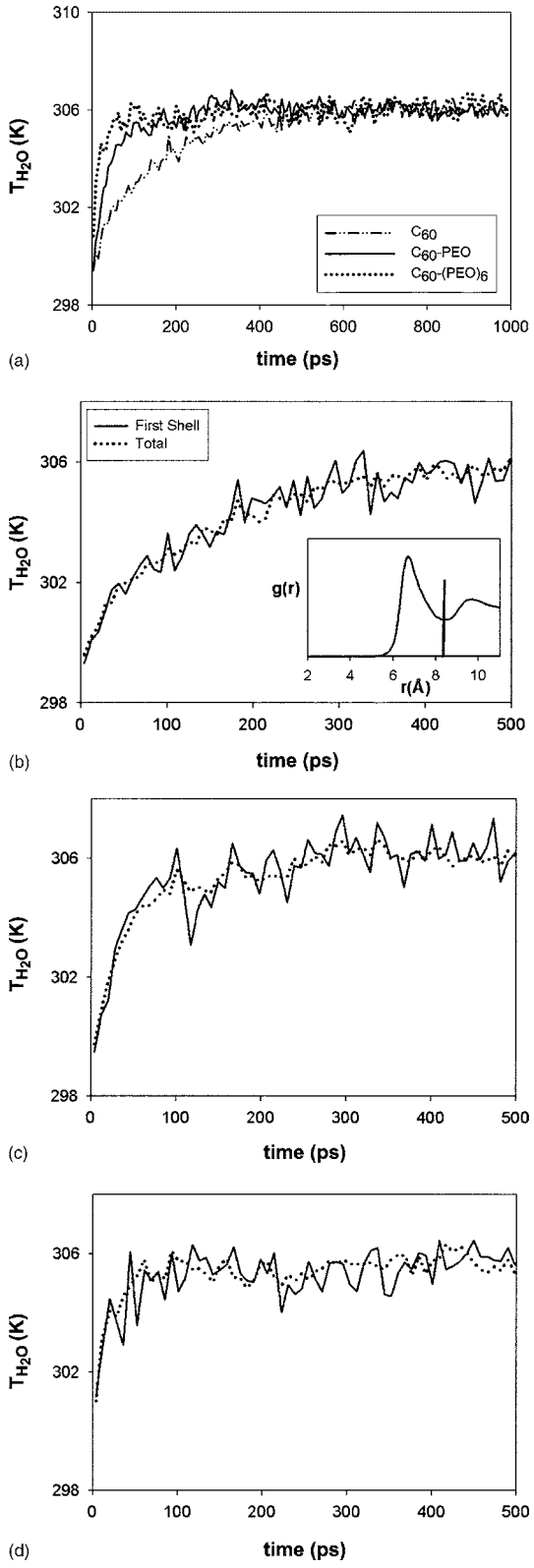

FIG. 3. (a) Temperature of water during the fullerene cooling process. Temperature of water in the first hydration shell during the fullerene cooling process of (b) C_{60}, (c) C_{60}-PEO, and (d) C_{60} -$(PEO)_6$ solutions during the fullerene cooling process. Hydration shells are shown in the inset to (b) which shows the pair distribution function of water with first hydration shell indicator relative to the center of mass of the fullerene.

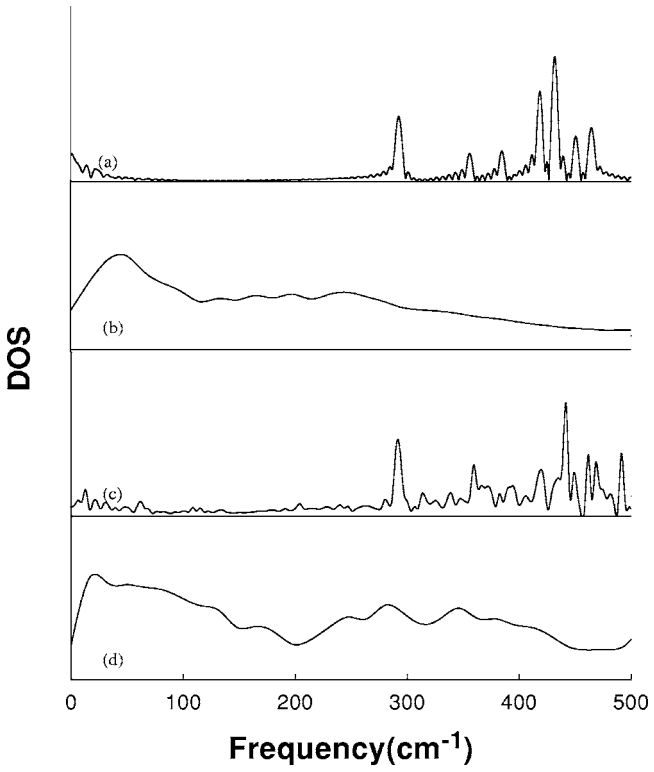

FIG. 4. Vibrational spectra of (a) C_{60}, (b) water, (c) C_{60} with six attached PEO chains (fullerene spectra only), and (d) attached PEO chains from simulations in aqueous solution.

vibrational cooling is transfer of energy from the fullerene to the attached PEO chains and not from PEO to the water.

IV. DISCUSSION AND CONCLUSIONS

Our molecular dynamics simulations reveal that vibrational cooling of unmodified single fullerenes in aqueous solution is an inefficient process due to little overlap of density of states between the fullerene and liquid water. The estimated interfacial conductance is about factor of 2 smaller than obtained in MD simulations of C_{84} relaxation in octane.[13] There are several factors that might be responsible for this difference. First, C_{60} due to its small size is characterized by very high frequency threshold for intramolecular vibrations, which for our model is slightly below 300 cm^{-1} [see Fig. 4(a)]. C_{84} is larger than C_{60} and consequently has a lower frequency threshold of intramolecular vibrations,[26] thus enhancing the coupling between internal C_{84} modes and the surrounding liquid vibrations. Second, the interactions between fullerenes and water or nonpolar liquid are via weak van der Waals forces. While octane molecules interact also via van der Waals forces, water-water interactions involve in addition much stronger dipolar forces. Thus we can expect a further limitation on the energy flow to water from C_{60} due to frequency mismatch associated with motion related to water-water and water-fullerene interactions.

Attachment of short PEO oligomers dramatically increases the interfacial conductance and decreases the vibrational relaxation time of C_{60} fullerenes. The dramatic de-

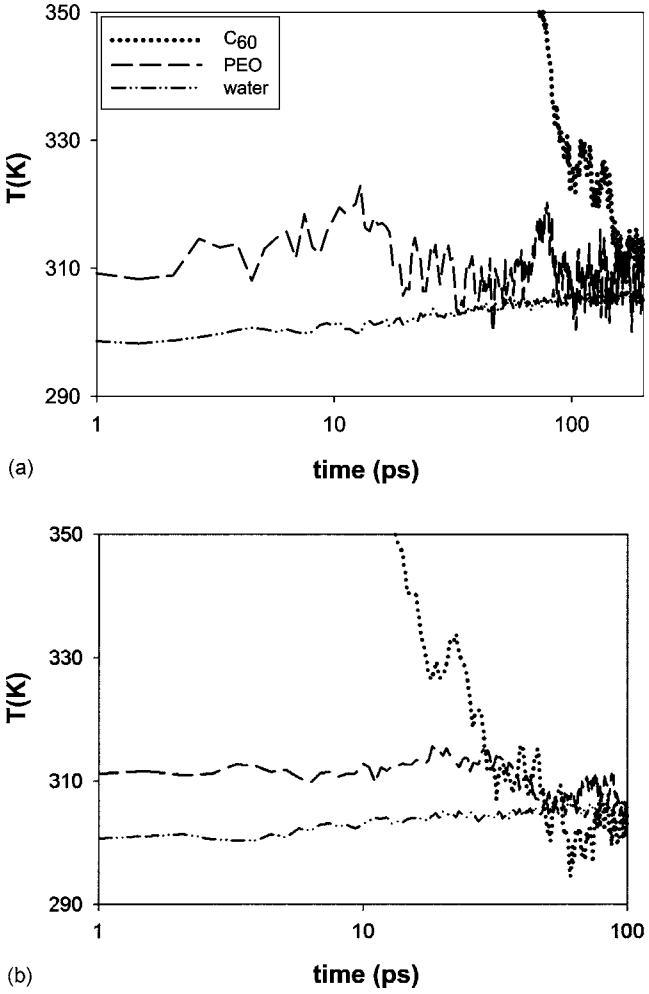

FIG. 5. The temperature of C_{60}, PEO, water and total system of (a) C_{60}-PEO and (b) C_{60}-$(PEO)_6$ solutions at short time range during the fullerene cooling process.

crease in the vibrational relaxation time of the fullerene by attachment of short polymer chains is likely due to the overlap in low-frequency density of states (soft phonons) between water and the attached chains. We anticipate that attachment of any conformational flexible group or chain with low-frequency anharmonic vibrational modes to fullerenes for the purpose of modifying their compatibility with water, their state of aggregation in water, or their interfacial, chemical or transport properties will have a similar effect on the vibrational relaxation of the fullerene.

Finally, while the vibrational cooling of C_{60} fullerenes with attached PEO chains can be interpreted in terms of transfer of vibrational energy from the fullerene to the low-frequency anharmonic modes of the PEO chains and from these modes to water, closer examination of Figs. 5(a) and 5(b) reveal that the process is complex. We observe a very rapid heating of the PEO chains on a time scale of less than 1 ps followed by slow additional heating of the PEO chain for 10–20 ps. Furthermore, simulations reveal that PEO segments nearer the fullerene (as measured along the chain from the attachment point) are more vibrationally excited at short times than those further from the fullerene. MD simulations of the vibrational cooling of PEO chains, shown in Fig. 2(b), reveal that when all vibrational modes (anharmonic and harmonic) of the chain are excited the vibrational relaxation time of PEO is approximately 11 ps, as given in Table III. Hence the vibrational temperature history of PEO during vibrational cooling of the fullerene can be interpreted as follows. Energy is transferred primarily from harmonic modes of the fullerene to harmonic modes of similar frequency associated with PEO segments attached to the fullerene. This energy is efficiently transferred to the surrounding water through the anharmonic PEO modes and less efficiently transferred to the higher frequency harmonic modes of the attached PEO segments and harmonic modes associated with PEO segments further along the chain(s). After 10–20 ps (corresponding to the vibrational relaxation time of the PEO chain) all modes of the PEO chain are excited and PEO reaches its maximum temperature. Now the anharmonic modes of the PEO chain must transfer energy from both the fullerene and the excited PEO chain to water. For C_{60}-PEO transferring energy from the PEO high-frequency modes to the PEO anharmonic modes and subsequently to water (τ =11 ps) is more efficient than transferring energy from the fullerene to the anharmonic modes of the single PEO chain and subsequently to water (τ=39 ps). Hence, the vibrational excitation of the PEO does not interfere significantly with the ability of the fullerene to lose energy through the PEO chain and the PEO temperature remains well below that of the fullerene. In contrast, for C_{60}-$(PEO)_6$ the fullerene and PEO temperatures are the same within the noise toward the end of the relaxation process, indicating that toward the end of the vibrational cooling process the process is limited by the ability of the PEO to transfer energy from the excited high frequency PEO modes to water (τ=11 ps) which is a less efficient process than transfer of energy from the fullerene to the PEO anharmonic modes and then to water (τ=7 ps). However, by the time PEO becomes vibrationally excited (around 10 ps) the fullerene has already lost most of its energy to water through the anharmonic modes of PEO and the vibrational excitation of the PEO influences only the tail of the fullerene cooling process.

ACKNOWLEDGMENTS

The authors would like to acknowledge support of the National Science Foundation through Grant No. ITR: CHE0312226.

[1] R. A. J. Janssen, J. C. Hummelen, and N. S. Sariciftci, MRS Bull. **30**, 33 (2005).
[2] R. A. Cheville and N. J. Halas, Phys. Rev. B **45**, R4548 (1992).
[3] S. B. Fleischer, E. P. Ippen, G. Dresselhaus, M. S. Dresselhaus, A. M. Rao, P. Zhou, and P. C. Eklund, Appl. Phys. Lett. **62**, 3241 (1993).
[4] V. M. Farztdinov, Y. E. Lozovik, Y. A. Matveets, A. G. Stepanov, and V. S. Letokhov, J. Phys. Chem. **98**, 3290 (1994).
[5] S. Ishihara, I. Ikemoto, S. Suzuki, K. Kikuchi, Y. Achiba, and T. Kobayashi, Chem. Phys. Lett. **295**, 475 (1998).
[6] T. Juhasz, X. H. Hu, C. Suarez, W. E. Bron, E. Maiken, and P. Taborek, Phys. Rev. B **48**, 4929 (1993).
[7] M. R. Wasielewski, M. P. O'Neil, K. R. Lykke, M. J. Pellin, and D. M. Gruen, J. Am. Chem. Soc. **113**, 2774 (1991).
[8] V. Klimov, L. Smilowitz, H. Wang, M. Grigorova, J. M. Robinson, A. Koskelo, B. R. Mattes, F. Wudl, and D. W. McBranch, Res. Chem. Intermed. **23**, 587 (1997).
[9] R. J. Sension, C. M. Phillips, A. Z. Szarka, W. J. Romanow, A. R. McGhie, J. P. McCauley, A. B. Smith, and R. M. Hochstrasser, J. Phys. Chem. **95**, 6075 (1991).
[10] T. W. Ebbesen, K. Tanigaki, and S. Kuroshima, Chem. Phys. Lett. **181**, 501 (1991).
[11] A. G. Stepanov, M. T. Portella-Oberli, A. Sassara, and M. Chergui, Chem. Phys. Lett. **358**, 516 (2002).
[12] H. S. Cho, T. K. Ahn, S. I. Yang, S. M. Jin, D. Kim, S. K. Kim, and H. D. Kim, Chem. Phys. Lett. **375**, 292 (2002).
[13] S. T. Huxtable, D. G. Cahill, S. Shenogin, and P. Keblinski, Chem. Phys. Lett. **407**, 129 (2005).
[14] E. Nakamura and H. Isobe, Acc. Chem. Res. **36**, 807 (2003).
[15] D. Bedrov, G. D. Smith, and L. Li, Langmuir **21**, 5251 (2005).
[16] D. Bedrov and G. D. Smith (unpublished).
[17] http://www.che.utah.edu/~gdsmith/mdcode/main.html
[18] U. Essmann, L. Perera, M. L. Berkowitz, T. Darden, H. Lee, and L. G. Pedersen, J. Chem. Phys. **103**, 8577 (1995).
[19] The classical harmonic heat capacity for a body with 84 unconstrained vibrational degrees of freedom, three translation degrees of freedom, and three rotational degrees of freedom is 0.173 kcal/mol/K.
[20] S. T. Huxtable, D. G. Cahill, S. Shenogin, L. Xue, R. Ozisik, P. Barone, M. Usrey, M. S. Strano, G. Siddons, M. Shim, and P. Keblinski, Nat. Mater. **2**, 731 (2003).
[21] Y. Deng and R. M. Stratt, J. Chem. Phys. **117**, 1735 (2002).
[22] C. Heidelbach, V. S. Vikhrenko, D. Schwarzer, I. I. Fedchenia, and J. Schroeder, J. Chem. Phys. **111**, 8022 (1999).
[23] D. Schwarzer, C. Hanisch, P. Kutne, and J. Troe, J. Phys. Chem. A **106**, 8019 (2002).
[24] J. Baier, P. Posch, G. Jungmann, H-W. Schmit, and A. Seilmeier, J. Chem. Phys. **114**, 6739 (2001).
[25] S. J. Woo, E. Kim, and Y. H. Lee, Phys. Rev. B **47**, 6721 (1993).
[26] I. Margiolaki, S. Margadonna, K. Prassides, S. Assimopoulos, K. P. Meletov, G. A. Kourouklis, T. J. S. Dennis, and H. Shinohara, Physica B **318**, 372 (2002).
[27] L. Li, D. Bedrov, and G. D. Smith, Phys. Rev. E **71**, 011502 (2005).
[28] J. H. Walther, R. Jaffe, T. Halicioglu, and P. Koumoutsakos, J. Phys. Chem. B **105**, 9980 (2001).
[29] Cerius2 http://www.accelrys.com/cerius2/
[30] G. D. Smith, O. Borodin, and D. Bedrov, J. Comput. Chem. **23**, 1480 (2002).
[31] W. L. Jorgensen, J. Chandrasekhar, J. D. Madura, R. W. Impey, and M. L. Klein, J. Chem. Phys. **79**, 926 (1983).
[32] M. P. Allen and D. J. Tildesley, *Computer Simulation of Liquids* (Clarendon, Oxford, 1989), p. 21.
[33] T. Werder, J. H. Walther, R. L. Jaffe, T. Halicioglu, and P. Koumoutsakos, J. Phys. Chem. B **107**, 1345 (2003).